FERMILAB-PUB-14-415-CD

Afterpulsing in Silicon Photomultipliers: Impact on the Phodotetectors Characterization

Adam Para

Fermi National Accelerator Laboratory, Batavia, IL60510,USA

Abstract

Novel generation of silicon-based photodetectors are attractive alternatives to the traditional phototubes. They offer significant advantages but they present new challenges too. Afterpulsing is an inrinsic property of the silicon detectors. Its influence on the observable characteristics of photodetectors is investigated within a simple statististal model.

Keywords: afterpulsing, photodetectors, excess noise factor

1. Introduction

Silicon photomultipliers (SiPM's, MPPC's) are the arrays of avalanche photodiodes operating in a Geiger mode. Their high gain, high detection efficiency and compact sizes in conjunction with very high pulse height resolution enabling 'photon counting' make them very attractive candidates for replacement of the traditional photomultipliers, PMTs, especially in applications where the total area of photodetectors required is small.

SiPM's offer several advantages over the PMT tubes but they also present new challenges related to solid state nature of these devices. Thermally generated free charge carriers create signals identical to those caused by photo-electrons, hence the dark count rates in typical devices are relatively large, in the range $10kHz - 1MHz/mm^2$[1].

Large number of carriers are present in the Geiger discharge; some of them may be trapped in metastable traps. Their subsequent release may produce additional pulses, afterpulses, which contribute to the observed signal. The stochastic nature of this process affects the performance of photodetectors.

2. Modeling of Afterpulses; Single Pulse

Afterpulses can be characterized in terms of the probability that a given pulse will produce a subsequent afterpulse and their time constant τ_{aft}. In this note the P_{aft} will be used to denote the average number of trapped electrons (hence the number ofafterpulses produced by a single pulse, not counting the next generation of afterpulses). For $P_{aft} \ll 1$ it has the meaning of the actual probability of producing an afterpulse. These parameters depend on the operating point of the SiPM. Increase of the bias voltage V_{bias} leads to corresponding increase of the P_{aft} because of the increase of the number of charge carriers in the avalanche $Q = C_{cell}(V_{bias} - V_{breakdown}) = C_{cell}V_{ov}$, where C_{cell} is the cell capacitance and the $V_{breakdown}$ is the breakdown voltage, and the simultaneous increase of the probability that a free charge carrier will initiate an avalanche, P_{Geiger}. The afterpulsing time constant τ_{aft} may depend on the temperature of the photodetector.

Operated by Fermi Research Alliance, LLC under Contract No. De-AC02-07CH11359 with the United States Department of Energy.

In general there might be several trapping levels present with different trapping probabilities and corresponding time constants. In the following we explore a simple model of one trapping level with a single afterpulsing probability and one time constant.

Afterpulsing is a stochastic process, the actual number of additional pulses undergoes fluctuations according to the Poisson distribution with P_{aft} being the expectation value. In the note the quantity P_{aft} will be referred to as 'afterpulsing probability'. Every afterpulse produces a standard avalanche, hence it may lead to a production of additional afterpulses.

In a realistic detector the situation is somewhat more complicated as the bias voltage after an avalanche drops to $V_{breakdown}$ and is being restored with the time constant τ_{RC} characteristic for a given device. Electrons released from the traps at timescales shorter than τ_{RC} have lower probability of producing an avalanche because of reduced P_{Geiger} and the charge of the avalanche will be reduced proportionally to the actual value of overvoltage, V_{ov}. The latter effect will lead to a reduced afterpulsing probability P_{aft} of the subsequent afterpulses regardless of their timing. These effects depend on the specific devices and they are ignored in the present study.

Afterpulsing is simulated assuming a single avalanche creating a Poisson-distributed number of afterpulses distributed with the exponential decay time. The procedure is iteratively applied to each of the generated afterpulses, thus leading to trains of pulses with varying numbers of pulses and theirt ime distributions.

3. Afterpulsing Pulse Rates; Effective Gain

Afterpulsing with fixed probability would lead to an increase of the number of pulses by an additional contribution of

$$N_{aft} = P_{aft} + P_{aft}^2 + P_{aft}^3 + ... = \frac{P_{aft}}{1 - P_{aft}} \tag{1}$$

and it may be treated as an additional gain factor, albeit dependent on the bias voltage. As shown in Fig.1 the same is true even in the case when the afterpulses are created with fluctuations governed by the Poisson statistics.

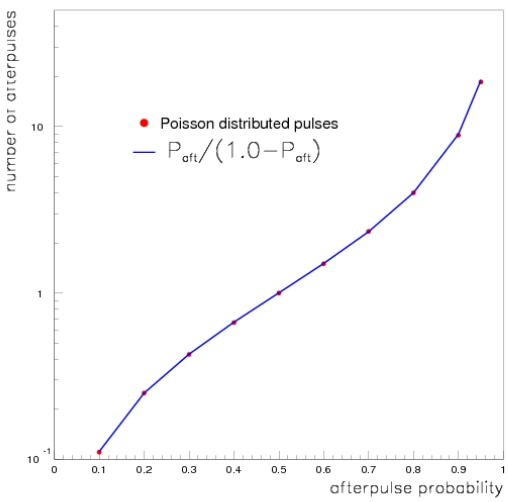

Figure 1: Average number of afterpulses as a function of the afterpulsing probability with the actual number of afterpulses undergoing statistical fluctuations.

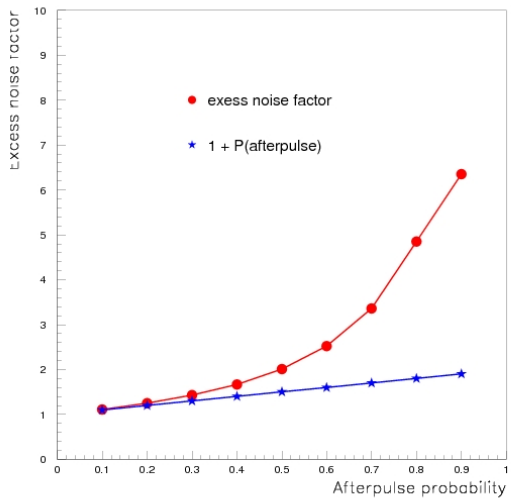

Figure 2: Excess noise factor as a function of the afterpulsing probability. For comparison a linear function $1 + P_{aft}$ is shown as a blue line.

The additional gain factor undergoes additional fluctuations thus it reduces the intrinsic resolution of the photodetector, which can be expressed in terms of the Excess Noise Factor, ENF[1]. Fig. 2 shows that the ENF grows very rapidly, much faster than linearly, with the P_{aft}.

[1]Excess noise factor is defined as $ENF = \frac{\sigma^2}{mean^2}$. For purely poissonian fluctuations $ENF = 1.0$. Any deviation of ENF from unity indicates additional fluctuations beyond purely statistical ones.

The increase of the number of additional pulses with P_{aft} (thus with V_{bias}) is the primary reason for the observed increase of the dark count rates with the bias voltage.

4. Afterpulses Time Distribution

Afterpulsing time constant can be determined experimentally by studying the observed time distribution of pulses following some 'trigger' pulse. An external light pulse can be used to provide the initial trigger and the contribution of thermal pulses can be subtracted. The shape of resulting time distribution is modified by the statistical nature of afterpulsing, however.

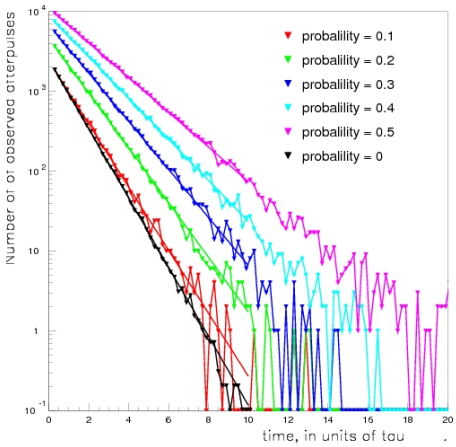

Figure 3: Time distribution, in units of τ_{RC}, of the observed pulses for aftepulses probability ranging from 0.1 to 0.5. The black distribution corresponds to the underlying exponential and no subsequent afterpulsing.

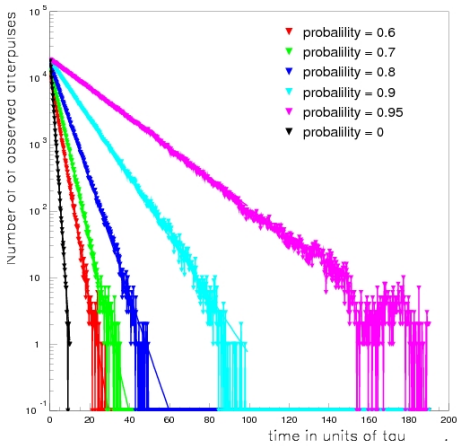

Figure 4: Time distribution, in units of τ_{RC}, of the observed pulses for aftepulses probability ranging from 0.6 to 0.95. The black distribution corresponds to the underlying exponential and no subsequent afterpulsing.

Figs. 3 and 4 illustrate the impact of subsequent afterpulsing on the time distribution of the observed pulses for different values of the P_{aft}. The time distribution of the observed pulses retains its exponential shape, but the characteristic time constant τ_{obs} grows with the afterpulsing probability, as shown in Fig. 5.

The value of τ_{obs} is a relevant parameter to describe the performance of a photodetector at the given operating conditions but it does not, in general, reflect the time constant of the underlying physics process, τ_{aft}. The latter can be determined better by studying the time distribution of the 'first' afterpulse. Such a method would yield a correct result in the case when the number of afterpulses to a given pulse is one. A Poisson nature of the number of produced afterpulses leads, however, to a systematic underestimate of the τ_{aft} as shown in Fig. 6.

5. Modeling of Afterpulses; Multiple Thermal Pulses

'Dark' pulses, i.e. pulses in the absence of the light signal consist of several components. The primary source of these pulses are the thermal excitations of free charge carriers leading to the avalanche process with the P_{Geiger} probability. The rate of these pulses depends on the temperature and the bias voltage, but the resulting pulses are randomly distributed in time with the overall rate

$$R(T, V_{ov}) = R_{thermal}(T) \times P_{Geiger}(V_{ov}) \tag{2}$$

where $R_{thermal}$ is a rate of thermally generated carriers at the temperature T.

The afterpulses (including the subsequent after-afterpulses) will increase the average rate of the observed pulses by a factor $1 + N_{aft}$ but the time structure of the resulting ensemble of pulses will be depend on the interplay between the afterpulsing time constant and the typical time distance between the thermal excitations $\Delta t_{thermal}$. The dark pulses

will be distributed randomly in time when $\Delta t_{thermal} \ll \tau_{aft}$ or there will be randomly distributed trains of pulses (with the train multiplicity and duration dependent on P_{aft}) when $\Delta t_{thermal} \gg \tau_{aft}$.

Thermally produced pulses have been generated in the interval $0 - 10\mu sec$ and the resulting afterpulses have been generated with the average multiplicity given by P_{aft} and time constant $\tau_{aft} = 50nsec$. Fig. 7 shows an example of the time distributions of pulses simulated with the thermal random rate of $2MHz$ and different afterpulsing probabilities. The apparent raise of the instantenous rate is a reflection of the lack of afterpulses corresponding to thermal pulses produced at $t < 0$. the time interval required to reach the asymptotic level in such a situation depends on the interplay of the afterpulsing time constant and the afterpulsing probability.

6. Thermal Pulses Rate Estimates

In the presence of afterpulses the observed 'dark' pulse rate is an overestimate of the rate of random thermal excitations by a factor $1 + N_{aft}$ which can exceed an order of magnitude. A better estimate of the initial thermal rate can be obtained from a distribution of pulses multiplicity in some time interval Δt. The probability of observation of zero pulses $P(0)$ in the given time interval provides an estimate of the average number of pulses expected in this time interval

$$< N >= -logP(0) \tag{3}$$

If there were no thermal pulses in the specific time interval then there will be no afterpulses either, therefore such method appears to be systematically superior to the use of the the raw observed rate. A possible presence of the afterpules to the pulses preceding the time interval in question reduces the probability of observing zero pulses and biases the resulting $< N >$ towards the higher values, however. To study the resulting bias the random thermal pulses were generated in the time interval of $10\mu sec$ with afterpulses corresponding to the time constant τ_{aft} of $50nsec$. To avoid an additional bias due to the imperfection of the simulation at the beginning of the simulated time interval the method was applied using variable gate length, all of the gates starting at $t = 7.5\mu sec$, well inside the steady state even for large afterpulsing probability, see Fig. 7.

Figs. 8 and 9 illustrate the magnitude of the systematic bias introduced by afterpulsing in the determination of the thermal pulses rates as a function of the of used gate length and the afterpulsing probability. For the gate length longer than $1\mu sec = 20\tau_{aft}$ the true thermal rate can be determined with the accuracy better than 20% even for very large afterpulsing probability.

7. Afterpulsing and Absolute Calibration

Absolute calibration of photodetectors, i.e. conversion of the observed signals into the number of photons impacting the photodetector, is the crucial step in several classes of experiments. One of they methods successfully used with photomultipliers involves illumination of the photodetector with a light signals of constant intensity and determination of the average number of photons impacting the photodetector from the width of the observed pulse height distribution using the Eq. 4

$$< N >= \frac{Mean^2}{RMS^2} \tag{4}$$

This method relies on the assumption that the variation of the observed signal is dominated by the Poisson fluctuations of the number of detected photons. It is a very good approximation for the PMT tubes, which have ENF very close to one. Fluctuations of afterpulsing contribute significantly (Fig. 2) to the fluctuations of the observed signals thus reducing the 'determined' number of the incident photons with respect to the true size of the photon signal. This effect can be parameterized as

$$< N^{det} >=< N^{true} > (1 - P_{aft}) \tag{5}$$

and it is illustrated in Fig. 10.

8. Summary

Afterpulsing is an intrinsic feature of SiPM-type photodetectors and it does contribute to the various factors relevant to the performance of these photodetectors. Proper inclusion of the afterpulsing in the analysis of the data is very important, but it depends on the properties of the photodetector (including the overall rate of afterpulsing and its time constant as well as the *RC* recharge time of the cells) as well as on the details of the experimental analysis (gate length). The results presented here can be used as a guidance to derive the corrections relevant for specific applications.

9. Acknowledgements

Fermi National Accelerator Laboratory is operated by Fermi Research Alliance, LLC under Contract No. DE-AC02-07CH11359 with the United States Department of Energy.

References

[1] http://www.hamamatsu.com/resources/pdf/ssd/mppc_kapd0002e.pdf

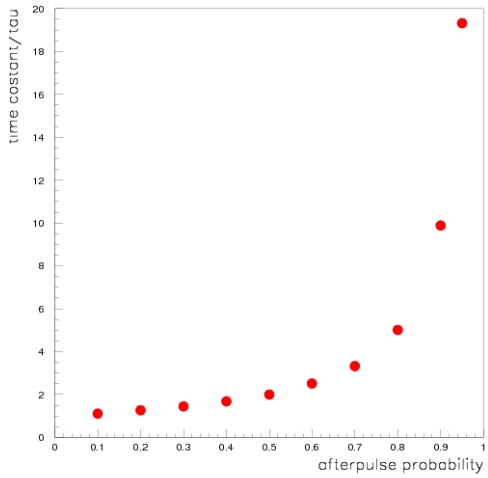

Figure 5: Effective afterpulsing time constant, in units of τ_{RC}, as a function of the afterpulsing probability.

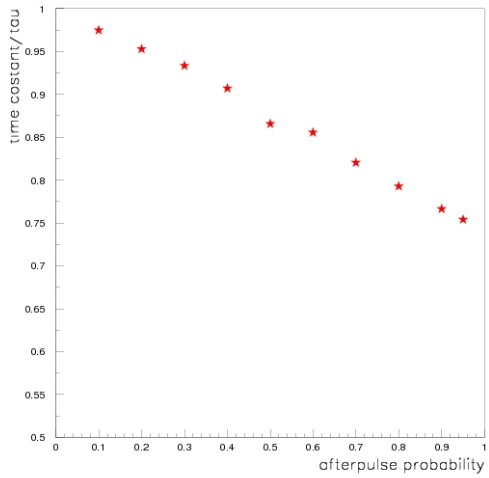

Figure 6: Time constant, in units of τ_{RC}, determined from the 'first afterpulse' as a function of the afterpulsing probability

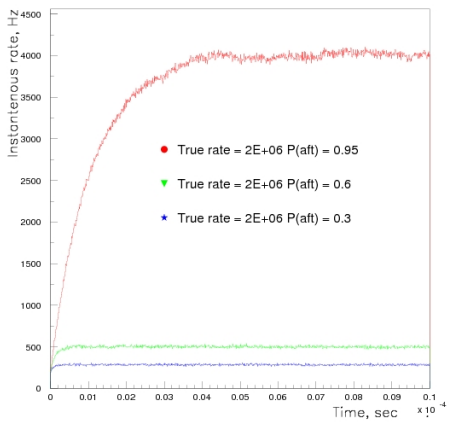

Figure 7: Instantenous rate as function of time after a 'turn-on' for different afterpulsing probabilities. The themral random rate is $2MHz$ and afterpulsing time constant is $50nsec$.

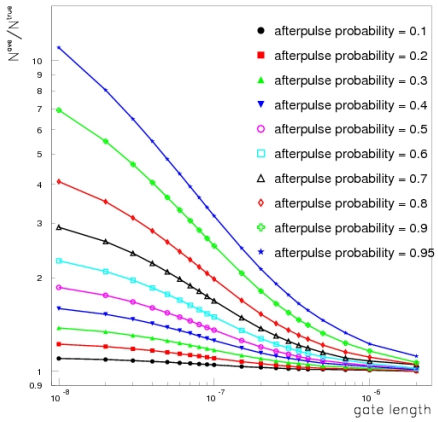

Figure 8: Ratio of the rate of thermal pulses estimated from the $P(0)$ to the true rate of the underlying thermal pulses for different afterpulsing probability P_{aft} as a function of the length of the time interval used.

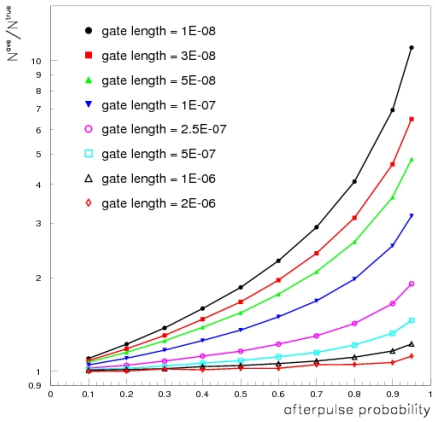

Figure 9: Ratio of the rate of thermal pulses estimated from the $P(0)$ to the true rate of the underlying thermal pulses for different time intervals as a function of afterpulsing probability.

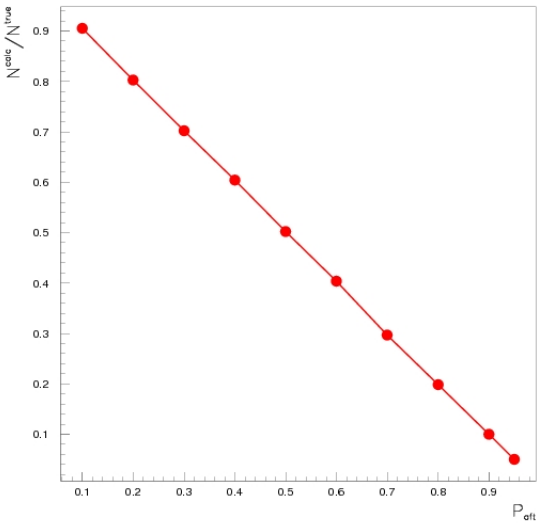

Figure 10: Reduction of size of the photon signal using the Eg.4 with respect to the truth as a function of Afterpulsing probabiluty.